Appl. Math. Mech. -Engl. Ed., **36**(3), 279–292 (2015)
DOI 10.1007/s10483-015-1912-6

Applied Mathematics and Mechanics (English Edition)

Vibration analysis and active control of nearly periodic two-span beams with piezoelectric actuator/sensor pairs*

Fengming LI[1,2,†], Zhiguang SONG[2]

1. College of Mechanical Engineering, Beijing University of Technology, Beijing 100124, China;
2. School of Astronautics, Harbin Institute of Technology, Harbin 150001, China

Abstract The piezoelectric materials are used to investigate the active vibration control of ordered/disordered periodic two-span beams. The equation of motion of each sub-beam with piezoelectric patches is established based on Hamilton's principle with an assumed mode method. The velocity feedback control algorithm is used to design the controller. The free and forced vibration behaviors of the two-span beams with the piezoelectric actuators and sensors are analyzed. The vibration properties of the disordered two-span beams caused by misplacing the middle support are also researched. In addition, the effects of the length disorder degree on the vibration performances of the disordered beams are investigated. From the numerical results, it can be concluded that the disorder in the length of the periodic two-span beams will cause vibration localizations of the free and forced vibrations of the structure, and the vibration localization phenomenon will be more and more obvious when the length difference between the two sub-beams increases. Moreover, when the velocity feedback control is used, both the forced and the free vibrations will be suppressed. Meanwhile, the vibration behaviors of the two-span beam are tuned.

Key words nearly periodic beam, vibration localization, active vibration control, piezoelectric material

Chinese Library Classification O342
2010 Mathematics Subject Classification 74K10

1 Introduction

Periodic structures (also called phononic crystals) are composed of identical sub-structures, and are designed and manufactured with certain regularity and periodicity. The periodic structures may contain certain small irregularities among the sub-structures because of manufacturing tolerances, material defects, and other factors, which may turn the ordered periodic structures into the disordered ones. Periodic structures possess the properties of frequency pass and stop bands, while disordered periodic structures have vibration and wave localization behaviors[1–3]. The vibration and wave behaviors of ordered and disordered periodic structures

* Received May 30, 2014 / Revised Jul. 23, 2014
Project supported by the National Basic Research Program of China (973 Program) (No. 2011CB711100) and the National Natural Science Foundation of China (Nos. 10672017 and 11172084)
† Corresponding author, E-mail: fmli@bjut.edu.cn

have received much attention in recent years[4–6]. Based on the dynamical advantages of such structures, they have been used to develop devices such as transducers and filters.

Recently, the vibration and wave propagation in ordered periodic structures and disordered periodic structures have been extensively studied[7–8]. Feng and Liu[9] studied the band-gap tuning of phononic crystals (steel/epoxy and aluminum/epoxy) with different initial stresses. The results showed that the initial stress could tune the location and width of the band-gap efficiently. Zhou and Chen[10] analyzed the effects of the initial stress on the band structures, and investigated the tunability of the band gaps of two locally resonant phononic crystals including the electroactive polymer layer by applying an electric field upon the electroactive layer. Su et al.[11] studied the variations of the frequency band gaps of one-dimensional functionally graded phononic crystals, and observed that the functionally graded material property played an important role in the band structures. Wang et al.[12] studied the wave propagation and localization in disordered layered three-component periodic structures with thermal effects, and showed that the incident angles, disorder degrees, thickness ratios, and temperature changes had prominent effects on the wave localization phenomena.

As a kind of popular intelligent materials, piezoelectric materials have been extensively used for the active vibration suppression of engineering structures. Senesi and Ruzzene[13] and Li and Wang[14] performed some attempts on the active tuning of wave propagation in ordered periodic structures and disordered periodic structures with the piezoelectric materials. Baz[15] studied the active control of wave propagation in periodic/aperiodic spring-mass structures with the piezoelectric actuators. Oh et al.[16] studied the active wave-guiding of a piezoelectric phononic crystal in a stop band frequency range, and analyzed the mechanism of the incident plane wave propagation through the waveguide. Wang et al.[17–18] designed the two- and three-dimensional phononic crystals with the piezoelectric and piezomagnetic inclusions, and studied the wave propagation properties with magneto-electro-elastic coupling. They found that piezoelectricity and piezomagneticity had remarkable effects on the frequency stop band behaviors.

Despite the recent progresses on the active tuning of wave propagation behaviors in ordered periodic structures by means of the piezoelectric materials, the active vibration control of finite periodic structures has seldom been studied. Therefore, we study the active vibration control in two-span ordered/disordered periodic beams with piezoelectric actuator/sensor pairs in this work. Hamilton's principle with an assumed mode method is used to establish the equation of motion of each sub-beam with piezoelectric patches. The active controller is designed by the velocity feedback control algorithm to obtain the active damping effect. Through calculating the free and forced vibration responses, the effects of the piezoelectric materials on the dynamical behaviors of the nearly periodic two-span beams are analyzed.

2 Structural equations of motion

A simply supported two-span beam with a constant thickness bonded with piezoelectric actuator/sensor pairs is considered. Figure 1 shows the Cartesian coordinates, in which the x-axis is on the neutral surface of the base beam and along the axial direction. The local coordinates of each span are also displayed in the figure (the positive direction of the x-axis for the left span is defined in the direction to the right, and it is defined in the direction to the left for the right span[19]). The middle support is misplaced with respect to its nominally symmetric position, and the misplacement is denoted by Δl. The total length, width, and thickness of the base beam are l, b, and h, respectively. The lengths of each span are

$$\begin{cases} l_1 = l/2 + \Delta l, \\ l_2 = l/2 - \Delta l. \end{cases}$$

The piezoelectric patches are well bonded at the middle points of the two spans on the

surface of the base beam, and they are positioned by the coordinates x_{10} and x_{20}. The length, width, and thickness of each piezoelectric actuator are l_{a}, b, and h_{a}, respectively, and the corresponding structural sizes for each piezoelectric sensor are l_{s}, b, and h_{s}, respectively. For small deformation, only the transverse deflection of the beam is considered.

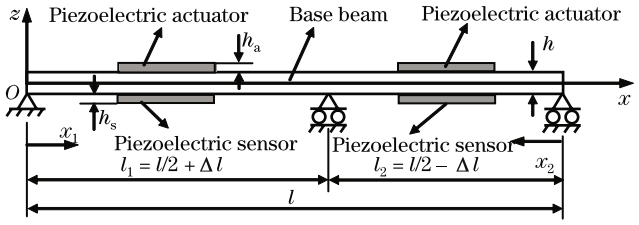

Fig. 1 Schematic diagram of two-span beam with piezoelectric patches

The base beam is homogeneous and isotropic, and the normal stress and strain in the axial direction are

$$\begin{cases} \sigma_x = E\varepsilon_x, \\ \varepsilon_x = -z\dfrac{\partial^2 w}{\partial x^2}, \end{cases} \tag{1}$$

where σ_x and ε_x are the normal stress and strain of the base beam in the x-direction, respectively, E is the elastic modulus of the base beam, and w is the transverse displacement of the beam.

The piezoelectric layer is transversely isotropic and polarized in the z-direction. The constitutive equations of the piezoelectric layer are expressed as[20–21]

$$\begin{cases} \sigma_x^{\mathrm{p}} = c_{11}\varepsilon_x - e_{31}E_z, \\ D_z = e_{31}\varepsilon_x + \epsilon_{33}E_z, \end{cases} \tag{2}$$

where c_{11}, e_{31}, and ϵ_{33} are the elastic constant, the piezoelectric constant, and the dielectric constant, respectively. σ_x^{p} is the normal stress in the x-direction. D_z is the electric displacement. E_z is the electric intensity in the z-direction, and it is denoted by[22–23]

$$E_z = V_0(t)/h_{\mathrm{p}},$$

where $V_0(t)$ is the external used voltage.

The transverse displacement of each sub-beam is expressed in terms of the generalized coordinates as follows:

$$\begin{aligned} w_k(x_k, t) &= \sum_{i=1}^{n} W_{ki}(x_k) r_{ki}(t) \\ &= \boldsymbol{W}_k^{\mathrm{T}}(x_k)\boldsymbol{r}_k(t), \end{aligned} \tag{3}$$

where $k = 1, 2$, n is the mode number, and $\boldsymbol{r}_k(t) = (r_{k1}, \cdots, r_{kn})^{\mathrm{T}}$ is the generalized coordinate vector. $\boldsymbol{W}_k(x_k) = (W_{k1}, \cdots, W_{kn})^{\mathrm{T}}$ is the principal vibration mode shape vector, which satisfies the geometric boundary conditions.

Then, based on Hamilton's principle with the assumed mode method, the equation of motion of each sub-beam with piezoelectric patches can be established as follows[24–27]:

$$\boldsymbol{M}_k\ddot{\boldsymbol{r}}_k(t)+\boldsymbol{K}_k\boldsymbol{r}_k(t)+\boldsymbol{K}_{Vk}V_{0k}(t)=F_k\boldsymbol{Q}_k, \tag{4}$$

where $k=1,2$, dot denotes the differentiation with respect to the time, $V_{0k}(t)$ is the external used voltage on the kth span, and F_k is the external transverse load used at x_{kF} of each span. $\boldsymbol{M}_k$, $\boldsymbol{K}_k$, $\boldsymbol{K}_{Vk}$, and $\boldsymbol{Q}_k$ are the modal mass matrix, the modal stiffness matrix, the electromechanical coupling vector, and the electromechanical forcing vector, respectively, which are expressed as follows:

$$\begin{aligned}\boldsymbol{M}_k=&\rho A\int_0^{l_k}\boldsymbol{W}_k\boldsymbol{W}_k^{\mathrm{T}}\mathrm{d}x_k\\&+\rho_{\mathrm{a}}A_{\mathrm{a}}\int_{x_{k0}-l_{\mathrm{a}}/2}^{x_{k0}+l_{\mathrm{a}}/2}\boldsymbol{W}_k\boldsymbol{W}_k^{\mathrm{T}}\mathrm{d}x_k\\&+\rho_{\mathrm{s}}A_{\mathrm{s}}\int_{x_{k0}-l_{\mathrm{s}}/2}^{x_{k0}+l_{\mathrm{s}}/2}\boldsymbol{W}_k\boldsymbol{W}_k^{\mathrm{T}}\mathrm{d}x_k,\end{aligned} \tag{5}$$

$$\begin{aligned}\boldsymbol{K}_k=&EI\int_0^{l_k}\frac{\mathrm{d}^2\boldsymbol{W}_k}{\mathrm{d}x_k^2}\frac{\mathrm{d}^2\boldsymbol{W}_k^{\mathrm{T}}}{\mathrm{d}x_k^2}\mathrm{d}x_k\\&+c_{11}b\Big(\frac{1}{4}h^2h_{\mathrm{a}}+\frac{1}{2}hh_{\mathrm{a}}^2+\frac{1}{3}h_{\mathrm{a}}^3\Big)\\&\cdot\int_{x_{k0}-l_{\mathrm{a}}/2}^{x_{k0}+l_{\mathrm{a}}/2}\frac{\mathrm{d}^2\boldsymbol{W}_k}{\mathrm{d}x_k^2}\frac{\mathrm{d}^2\boldsymbol{W}_k^{\mathrm{T}}}{\mathrm{d}x_k^2}\mathrm{d}x_k\\&+c_{11}b\Big(\frac{1}{4}h^2h_{\mathrm{s}}+\frac{1}{2}hh_{\mathrm{s}}^2+\frac{1}{3}h_{\mathrm{s}}^3\Big)\\&\cdot\int_{x_{k0}-l_{\mathrm{s}}/2}^{x_{k0}+l_{\mathrm{s}}/2}\frac{\mathrm{d}^2\boldsymbol{W}_k}{\mathrm{d}x_k^2}\frac{\mathrm{d}^2\boldsymbol{W}_k^{\mathrm{T}}}{\mathrm{d}x_k^2}\mathrm{d}x_k,\end{aligned} \tag{6}$$

$$\boldsymbol{K}_{Vk}=\frac{1}{2}e_{31}b(h+h_{\mathrm{a}})\int_{x_{k0}-l_{\mathrm{a}}/2}^{x_{k0}+l_{\mathrm{a}}/2}\frac{\mathrm{d}^2\boldsymbol{W}_k^{\mathrm{T}}}{\mathrm{d}x_k^2}\mathrm{d}x_k, \tag{7}$$

$$\boldsymbol{Q}_k=\boldsymbol{W}^{\mathrm{T}}(x_{kF}), \tag{8}$$

where $k=1,2$. x_{k0} $(k=1,2)$ are the coordinates for the center points of the piezoelectric patches. ρ, ρ_{a}, and ρ_{s} are the mass densities of the base beam, the piezoelectric actuators, and the sensors, respectively. A, A_{a}, and A_{s} are the areas of the cross sections of the beam, the piezoelectric actuators, and the sensors, respectively. I is the inertia moment of the cross section of the base beam. For the beam with a rectangular cross section (see Fig. 1),

$$I=bh^3/12.$$

For the beam with the circular cross section,

$$I=\pi d^4/64,$$

where d is the diameter of the circular cross section of the beam. For the detailed derivation process of Eq. (4), one can refer to Ref. [26] and Ref. [27].

To analyze the dynamical properties of the beam with the piezoelectric patches, the formulation of the principal mode shape $\boldsymbol{W}_k(x_k)$ in Eq. (3) must be presented. For the simply supported two-span beam (see Fig. 1), according to the deducing process mentioned in Ref. [19], the mode shape for the transverse displacement of each sub-beam can be derived. By means of the methodology in Ref. [19], based on the equation of motion of each span and the boundary conditions of the three simple supports, the mode shapes $W_{ki}(x_k)$ $(i = 1, 2, \cdots, n)$ for the simply supported two-span beam can be deduced as follows:

$$W_{1i}(x_1) = -\frac{\sinh(\beta_i l_1)}{\sin(\beta_i l_1)} \sin(\beta_i x_1) + \sinh(\beta_i x_1), \quad 0 \leqslant x_1 \leqslant l_1, \tag{9}$$

$$W_{2i}(x_2) = -\frac{\sinh(\beta_i l_1)}{\sin(\beta_i l_2)} \sin(\beta_i x_2) + \frac{\sinh(\beta_i l_1)}{\sinh(\beta_i l_2)} \sinh(\beta_i x_2), \quad 0 \leqslant x_2 \leqslant l_2, \tag{10}$$

where β_i $(i = 1, 2, \cdots, n)$ can be determined by the following characteristic equation:

$$\frac{\cosh(\beta_i l_1)}{\sinh(\beta_i l_1)} + \frac{\cosh(\beta_i l_2)}{\sinh(\beta_i l_2)} - \frac{\cos(\beta_i l_2)}{\sin(\beta_i l_2)} - \frac{\cos(\beta_i l_1)}{\sin(\beta_i l_1)} = 0. \tag{11}$$

In the above equations,

$$\beta_i = (\omega_i/\alpha)^{1/2},$$

where ω_i is the natural frequency, and

$$\alpha = (EI/(\rho A))^{1/2}.$$

Equation (11) is a transcendental equation for β_i. It can only be solved by numerical methods. For the detailed deducing process of Eqs. (9) and (10), one may refer to Ref. [19].

3 Design of controllers

To suppress the vibration of the nearly periodic two-span beam, the velocity feedback control algorithm is used to obtain the active damping effect. The charges will be generated by the deformations of the piezoelectric sensors when the external dynamic loads are used to the sensors, and they can be written as follows[28–29]:

$$\begin{aligned} Q_{\mathrm{s}k}(t) &= \int_{S_{k(z=z_{ck})}} D_z \mathrm{d}S_k \\ &= -e_{31} b \int_{x_{k0}-l_{\mathrm{s}}/2}^{x_{k0}+l_{\mathrm{s}}/2} z_{ck} \frac{\mathrm{d}^2 \boldsymbol{W}_k^{\mathrm{T}}}{\mathrm{d}x_k^2} \mathrm{d}x_k \\ &= \boldsymbol{K}_{\mathrm{s}k} \boldsymbol{r}_k(t), \end{aligned} \tag{12}$$

where $k = 1, 2$. S_k is the surface area of the kth sensor, z_{ck} is the transverse coordinate of the mid-surface of the kth piezoelectric sensor from the neutral surface of the base beam, and $\boldsymbol{K}_{sk}$ can be written as follows:

$$\boldsymbol{K}_{\mathrm{s}k} = \frac{1}{2} e_{31} b (h + h_{\mathrm{s}}) \int_{x_{k0}-l_{\mathrm{s}}/2}^{x_{k0}+l_{\mathrm{s}}/2} \frac{\mathrm{d}^2 \boldsymbol{W}_k^{\mathrm{T}}}{\mathrm{d}x_k^2} \mathrm{d}x_k. \tag{13}$$

The sensing voltage V_{sk} can be calculated by the following expression[30–31]:

$$V_{\mathrm{s}k} = \frac{Q_{\mathrm{s}k}}{C_{\mathrm{s}k}}, \tag{14}$$

where C_{sk} is the capacitance of the kth piezoelectric sensor defined by[32]

$$C_{sk} = \frac{\epsilon_{33} S_k}{h_s}. \tag{15}$$

Substituting Eqs. (12) and (15) into Eq. (14), the sensing voltage can be expressed as follows:

$$V_{sk} = \boldsymbol{B}_k \boldsymbol{r}_k(t), \tag{16}$$

where the coefficient vector $\boldsymbol{B}_k$ can be written as follows:

$$\boldsymbol{B}_k = \frac{\boldsymbol{K}_{sk} h_s}{\epsilon_{33} S_k}. \tag{17}$$

When the velocity feedback controller is designed, the control voltage exerted on the piezoelectric actuator can be written as[29]

$$V_{0k}(t) = G_k \dot{V}_{sk}(t), \tag{18}$$

where G_k is the feedback control gain for the piezoelectric actuators. Substituting Eq. (16) into Eq. (18) yields the control voltage as follows:

$$V_{0k}(t) = G_k \boldsymbol{B}_k \dot{\boldsymbol{r}}_k(t). \tag{19}$$

Substituting Eq. (19) into Eq. (4) yields the equation of motion of each sub-beam with piezoelectric patches as follows:

$$\boldsymbol{M}_k \ddot{\boldsymbol{r}}_k(t) + \boldsymbol{C}_k \dot{\boldsymbol{r}}_k(t) + \boldsymbol{K}_k \boldsymbol{r}_k(t) = F_k \boldsymbol{Q}_k, \tag{20}$$

where $\boldsymbol{C}_k$ is the active damping matrix due to the piezoelectric actuator expressed by

$$\boldsymbol{C}_k = G_k \boldsymbol{K}_{Vk} \boldsymbol{B}_k. \tag{21}$$

It is observed from Eq. (20) that the velocity feedback control algorithm can provide active damping effects to the structure. Therefore, it can actively control the dynamical properties of the nearly periodic two-span beams.

By calculating the eigenvalue problem of the two-span beam with the piezoelectric actuator/sensor pairs, we can obtain the natural frequencies of the structural system. The general solution of the homogeneous differential equation of Eq. (20) can be written as

$$\boldsymbol{r}(t) = (\boldsymbol{r}_1^{\mathrm{T}}(t), \boldsymbol{r}_2^{\mathrm{T}}(t))^{\mathrm{T}} = \boldsymbol{r}_0 \mathrm{e}^{\lambda t}, \tag{22}$$

where $\boldsymbol{r}_0$ and λ are the eigenvector and the eigenvalue, respectively. Substituting Eq. (22) into the homogeneous differential equation of the whole structural system yields the following eigenvalue problem:

$$(\boldsymbol{M}\lambda^2 + \boldsymbol{C}\lambda + \boldsymbol{K})\boldsymbol{r}_0 = 0, \tag{23}$$

where

$$\begin{cases} \boldsymbol{M} = \begin{pmatrix} \boldsymbol{M}_1 & 0 \\ 0 & \boldsymbol{M}_2 \end{pmatrix}, \\ \boldsymbol{C} = \begin{pmatrix} \boldsymbol{C}_1 & 0 \\ 0 & \boldsymbol{C}_2 \end{pmatrix}, \\ \boldsymbol{K} = \begin{pmatrix} \boldsymbol{K}_1 & 0 \\ 0 & \boldsymbol{K}_2 \end{pmatrix}. \end{cases} \tag{24}$$

To satisfy the condition for getting a non-trivial solution of Eq. (23), the coefficient determinant of Eq. (23) must be zero, i.e.,

$$\left|\boldsymbol{M}\lambda^2 + \boldsymbol{C}\lambda + \boldsymbol{K}\right| = 0. \tag{25}$$

Then, the eigenvalues can be obtained. The imaginary parts of the eigenvalues are the natural frequencies of the whole structural system. In the next section, the free and forced vibrations are considered to investigate the effects of the piezoelectric materials on the dynamical behaviors of the nearly periodic two-span beams.

4 Numerical examples and discussion

4.1 Validation

In this section, the comparisons with the results available in the open literatures are made to validate the present methodology. The material and structural parameters for a uniform and circular Euler-Bernoulli beam are[33]

$$\begin{cases} E = 2.069 \times 10^{11}\,\mathrm{N}\cdot\mathrm{m}^{-2}, \\ \rho A = 15.387\,5\,\mathrm{kg}\cdot\mathrm{m}^{-1}, \\ I = 3.067\,96 \times 10^{-7}\,\mathrm{m}^4, \\ d = 0.05\,\mathrm{m}, \quad l = 1\,\mathrm{m}, \quad l_1 = 0.4\,\mathrm{m}, \end{cases}$$

where E is Young's modulus, ρ is the mass per unit length, d is the diameter, I is the inertia moment of the cross-sectional area, l is the total length, and l_1 is the length of the first span.

To validate the formulation developed by Hamilton's principle with the assumed mode method and the MATLAB codes, the natural frequencies of the two-span beam without piezoelectric patches are calculated and compared with the results of Lin and Tsai[33] and the results obtained by the finite element method (FEM) with the ANSYS software (see Table 1). From the table, it can be seen that the natural frequencies obtained by the present method are in good agreement with those in the open literature and obtained by the FEM, which verifies the validity of the present methodology.

Table 1 Comparisons of natural frequencies ($\mathrm{rad}\cdot\mathrm{s}^{-1}$) of two-span beam without piezoelectric patches

Method	Mode sequence number				
	1	2	3	4	5
Ref. [33]	2 147.673 5	4 937.511 0	8 219.970 5	15 847.505 4	19 288.538 8
FEM	2 142.629 0	4 921.440 3	8 192.008 2	15 750.883 6	18 901.078 0
Present	2 147.673 9	4 937.510 2	8 219.970 4	15 847.506 0	19 288.543 1

4.2 Analysis and active control of free vibration

Based on the verification, we carry out a free vibration analysis for the two-span beams in this section. The structural sizes and the material properties of the beam and piezoelectric

materials are

$$\begin{cases} l = 1\,\mathrm{m}, \quad l_\mathrm{a} = l_\mathrm{s} = 0.2\,\mathrm{m}, \\ b = h = 0.05\,\mathrm{m}, \quad h_\mathrm{a} = h_\mathrm{s} = 0.001\,\mathrm{m}, \\ E = 2.069 \times 10^{11}\,\mathrm{N \cdot m^{-2}}, \\ E_\mathrm{a} = E_\mathrm{s} = 69 \times 10^{9}\,\mathrm{N \cdot m^{-2}}, \\ \rho = 7\ 830\,\mathrm{kg \cdot m^{-3}}, \quad e_{31} = 22.86\,\mathrm{c \cdot m^{-2}}, \\ \rho_\mathrm{a} = \rho_\mathrm{s} = 7\ 600\,\mathrm{kg \cdot m^{-3}}, \quad \epsilon_{33} = 1.5 \times 10^{-8}\,\mathrm{F \cdot m^{-1}}, \end{cases}$$

where E_a and E_s are Young's moduli of the piezoelectric actuator and sensor, respectively. In the free vibration of the two-span beam, the external transverse loads F_1 and F_2 are firstly exerted on the mid-points of each span of the two-span beam during a very short time span, i.e., 0.001 s, and then the beam undergoes the free vibration without any external load. The amplitudes of F_1 and F_2 are both 1 N. In this section, in order to investigate the forced vibration of the structural system more conveniently, a decibel calculation is carried out on the displacement w, and the obtained result is noted by w_d.

First of all, the ordered two-span periodic beam is studied. The lengths of the two spans are equal. The free vibration responses of the symmetric points on the two sub-beams are computed and shown in Fig. 2. It can be seen from the figure that the vibrations of the symmetric points on the two-span beam are totally the same.

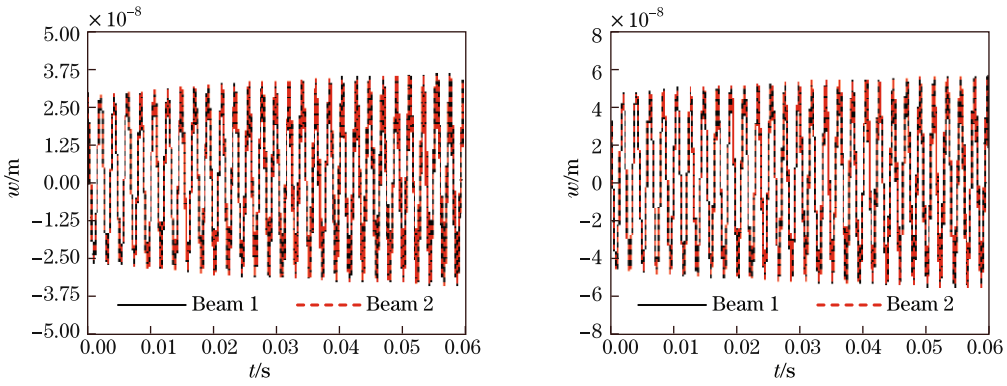

Fig. 2 Free vibration responses of symmetric points on each span of ordered two-span beam

Then, the disordered two-span beam is analyzed. The misplacement Δl is −0.1 m, and thus the lengths of the left span (Beam 1) and the right span (Beam 2) are 0.4 m and 0.6 m, respectively. The free vibration responses of two pairs of symmetric points ($x_1 = x_2 = 0.1\,\mathrm{m}$ and $x_1 = x_2 = 0.3\,\mathrm{m}$) on the two spans are computed and displayed in Fig. 3. It is observed from the figure that the free vibrations of the symmetric points on the disordered two-span beam are no longer the same, including the vibration amplitude and the natural frequency. Moreover, the amplitude of the right span (Beam 2) is larger.

Next, the effects of the disorder degree on the vibration characteristics of the nearly periodic two-span beam are investigated. The free vibration responses of the symmetric points on the

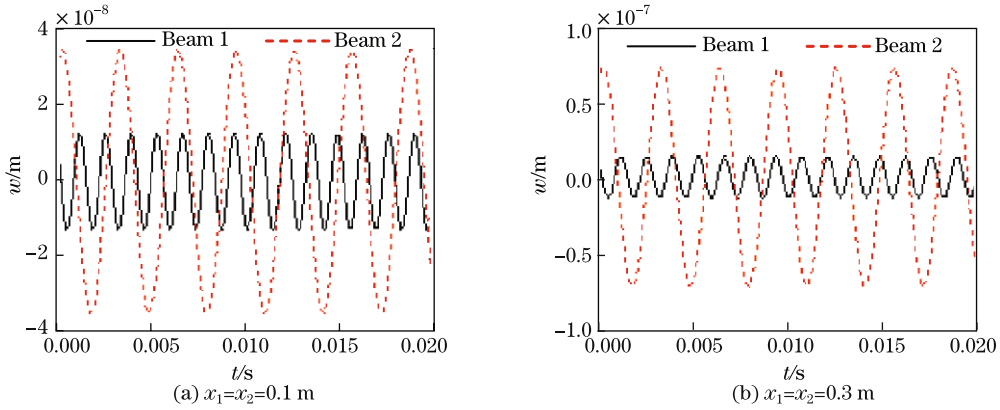

Fig. 3 Free vibration responses of symmetric points on disordered two-span beam

disordered two-span beam with different misplacements of the middle support are shown in Fig. 4. It is obvious that the vibration amplitude difference between the two symmetric points on the two spans increases with the increase in the length difference between the left and right spans.

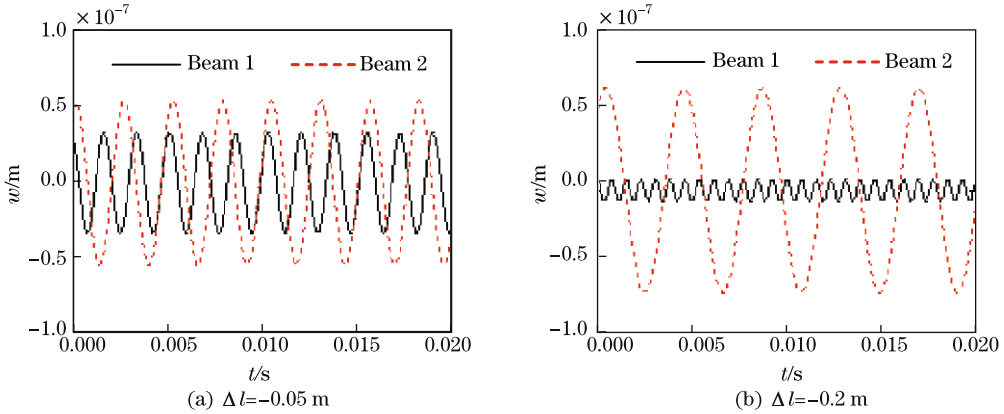

Fig. 4 Free vibration responses of symmetric points on disordered two-span beam with different misplacements of middle support, where $x_1 = x_2 = 0.2$ m

Finally, the active vibration control is carried out. The results of the controlled time histories and the controlled actuator voltages for the ordered periodic two-span structural system are shown in Fig. 5. It is observed from the figure that the vibrations of the structural system are convergent after being controlled by the velocity feedback controller, and the control voltages used in the control process are relatively low, which indicates that the velocity feedback control method is efficient in the active vibration control of ordered two-span beams.

The results of the controlled time histories and the controlled actuator voltages for the disordered structural system are displayed in Fig. 6. It is seen from Fig. 6(a) that, when the velocity feedback control is used, the free vibration will be convergent. Therefore, the vibration of the disordered beam is suppressed, and to some extent, the vibration localization of the two-span beam is tuned. From Fig. 6(b), we can see that the control voltages of the two actuators are also low.

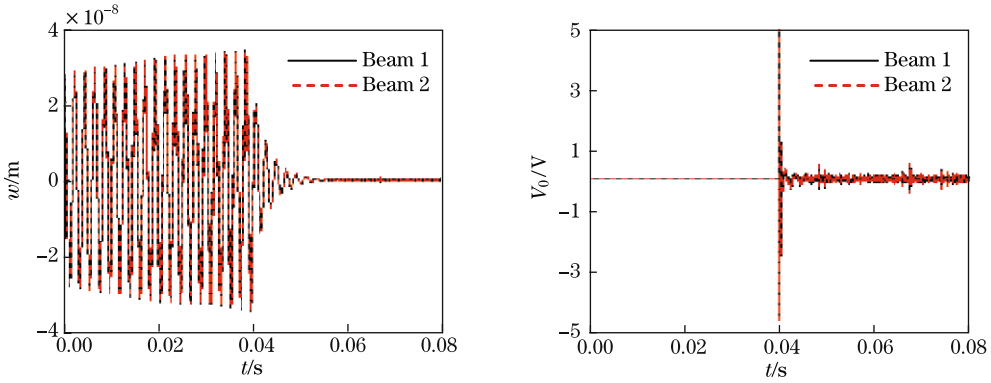

(a) Time histories (b) Voltages

Fig. 5 Controlled time histories and voltages of symmetric points on ordered two-span beam, where $x_1 = x_2 = 0.1\,\mathrm{m}$ and $G_1 = G_2 = 0.01$

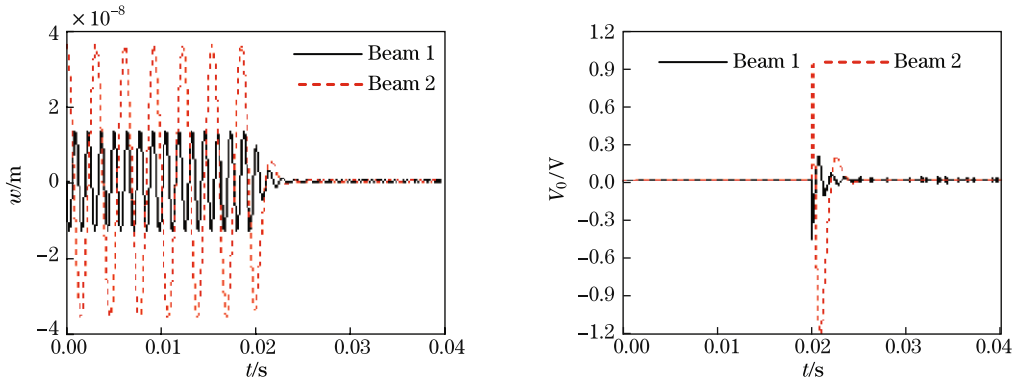

(a) Time histories (b) Voltages

Fig. 6 Controlled time histories and voltages of symmetric points on disordered two-span beam, where $x_1 = x_2 = 0.1\,\mathrm{m}$, $G_1 = 0.01$, and $G_2 = 0.08$

4.3 Analysis and active control of forced vibration

In this section, the forced vibration properties of the ordered and disordered two-span beams are investigated. The structural sizes and material properties are the same as those in the above section. The external loads F_1 and F_2 are both sinusoidal excitations.

First of all, the ordered two-span beam is studied. Figure 7 shows the forced vibration amplitudes of the transverse displacements of the symmetric points at $x_1 = x_2 = 0.1\,\mathrm{m}$, varying with the frequency of the external load. It is noted that the forced vibration responses of the symmetric points on the two sub-beams are totally the same for the ordered periodic two-span beam. It is a similar conclusion to that of the free vibration for the ordered two-span beam. Then, the forced vibration of the disordered beam is researched. The forced vibration responses of two pairs of symmetric points ($x_1 = x_2 = 0.1\,\mathrm{m}$ and $x_1 = x_2 = 0.3\,\mathrm{m}$) are displayed in Fig. 8. It is seen from the figure that the natural frequencies and the vibration amplitudes of the symmetric points on the disordered two-span beam are different.

Next, the effects of the disorder degree on the forced vibration characteristics of the disordered two-span structural system are investigated. The results show that the natural frequency difference between the two spans increases with the increase in the misplacement of the middle support (see Fig. 9).

Finally, the velocity feedback control is used. The controlled results are shown in Fig. 10.

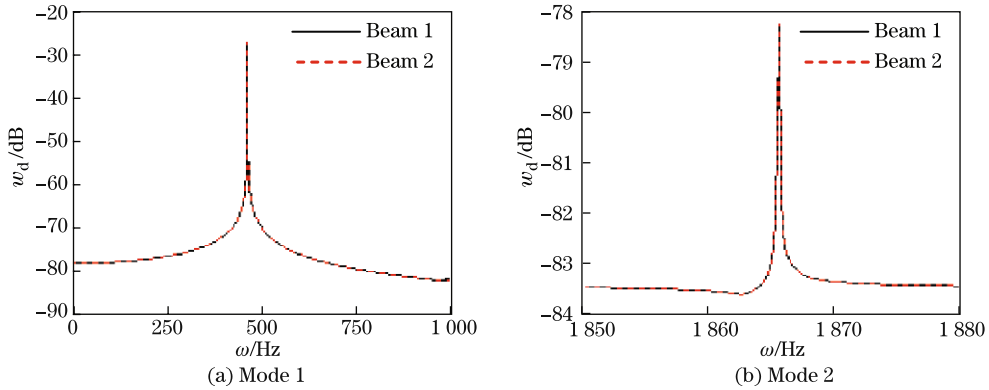

Fig. 7 Forced vibration responses of symmetric points on ordered two-span beam, where $x_1 = x_2 = 0.1\,\mathrm{m}$ and $l_1 = l_2 = 0.5\,\mathrm{m}$

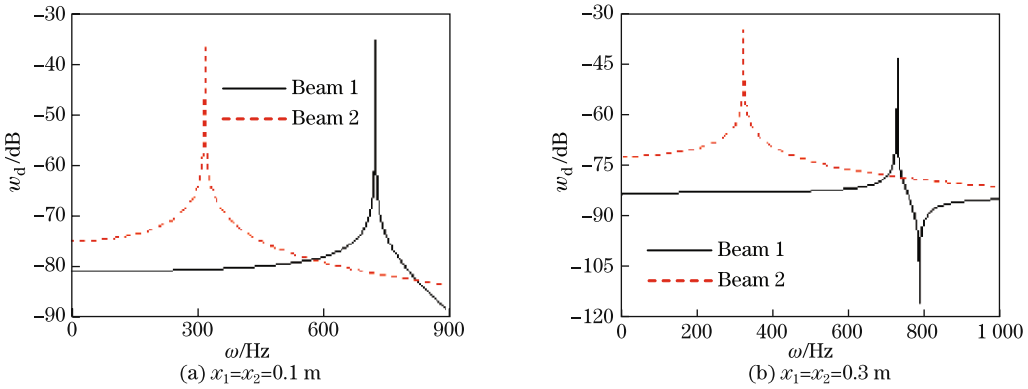

Fig. 8 Forced vibration responses of symmetric points on disordered two-span beam, where $l_1 = 0.4\,\mathrm{m}$

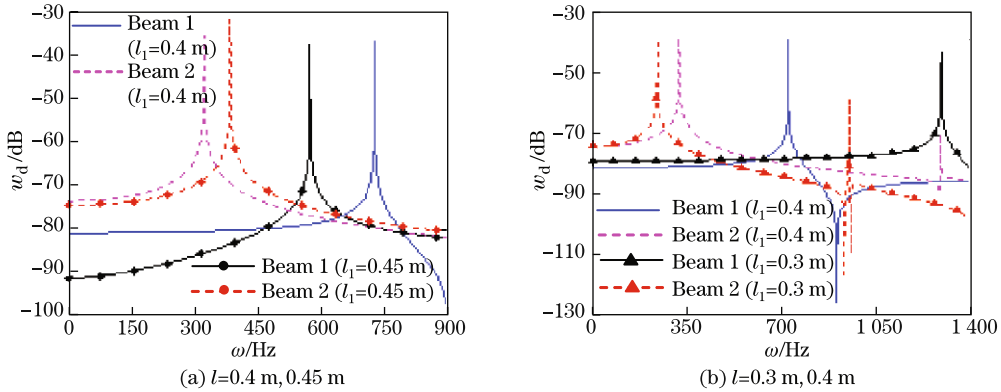

Fig. 9 Forced vibration responses of symmetric points on disordered two-span beam with different misplacements of middle support, where $x_1 = x_2 = 0.2\,\mathrm{m}$

It is seen from the figure that after the active control is used, the forced vibration amplitude decreases, and the vibration localization of the two-span beam is tuned. The control voltages used in the active control are very low.

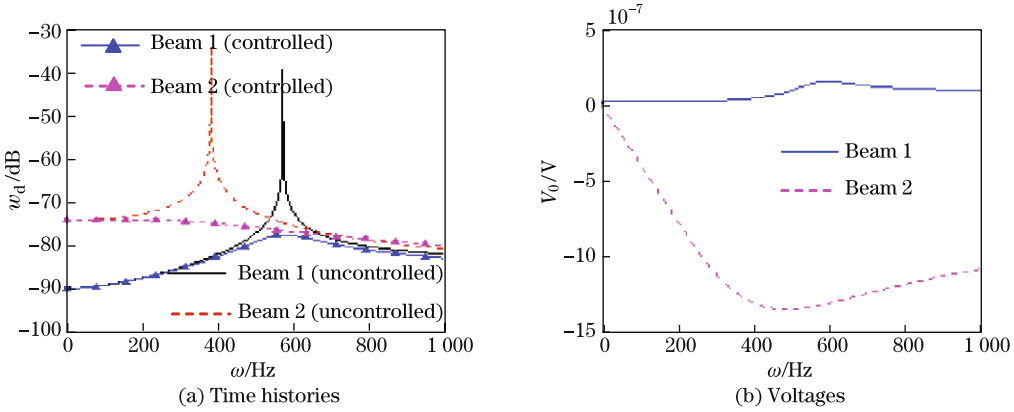

(a) Time histories (b) Voltages

Fig. 10 Controlled vibration responses and voltages of symmetric points on disordered two-span beam, where $l_1 = 0.45$ m, $G_1 = 0.01$, and $G_2 = 0.08$

5 Conclusions

The free and forced vibration behaviors of the ordered and disordered periodic two-span beams are investigated. The active vibration control for the two-span structure is also carried out. Hamilton's principle and the assumed mode method are used to establish the equation of motion. The active controller is designed by the velocity feedback control algorithm. The vibration characteristics of the ordered and disordered two-span beams are analyzed. The effects of the disorder degree on the vibration performances of the beam are investigated. The controlled effects of the velocity feedback controller on the vibration of the two-span beam are also studied. From the numerical simulation, the following conclusions can be drawn:

(i) In the ordered periodic two-span beam, the vibrations of the symmetric points on the two spans are totally the same. However, if the middle support is misplaced, the original ordered two-span beam will be disordered, and the vibrations of the symmetric points are no longer the same, i.e., the vibration localization occurs.

(ii) When the misplacement of the middle support increases, the differences of the vibration amplitude and the natural frequency between the two spans increase, and thus the vibration localization of the two-span beam becomes more and more obvious.

(iii) The velocity feedback controller is efficient in the active vibration control of the two-span beam. Meanwhile, the vibration localization is tuned to some extent.

References

[1] Huang, B. W. and Kuang, J. H. Mode localization in a rotating mistuned turbo disk with Coriolis effect. *International Journal of Mechanical Sciences*, **43**, 1643–1660 (2001)

[2] Sharma, D., Gupta, S. S., and Batra, R. C. Mode localization in composite laminates. *Composite Structures*, **94**, 2620–2631 (2012)

[3] Yan, Z. Z., Zhang, C., and Wang, Y. S. Analysis of wave propagation and localization in periodic/disordered layered composite structures by a mass-spring model. *Applied Physics Letters*, **94**, 161909 (2009)

[4] Yan, Z. Z., Zhang, C., and Wang, Y. S. Attenuation and localization of bending waves in a periodic/disordered fourfold composite beam. *Journal of Sound and Vibration*, **327**, 109–120 (2009)

[5] Li, F. M., Wang, Y. S., Hu, C., and Huang, W. H. Localization of elastic waves in periodic rib-stiffened rectangular plates under axial compressive load. *Journal of Sound and Vibration*, **281**, 261–273 (2005)

[6] Liu, Y., Su, J. Y., and Gao, L. T. The influence of the micro-topology on the phononic band gaps in 2D porous phononic crystals. *Physics Letters A*, **372**, 6784–6789 (2008)

[7] Matar, O. B., Robillard, J. F., Vasseur, J. O., Hladky-Hennion, A. C., Deymier, P. A., Pernod, P., and Preobrazhensky, V. Band gap tunability of magneto-elastic phononic crystal. *Journal of Applied Physics*, **111**, 054901 (2012)

[8] Robillard, J. F., Matar, O. B., Vasseur, J. O., Deymier, P. A., Stippinger, M., Hladky-Hennion, A. C., Pennec, Y., and Djafari-Rouhani, B. Tunable magnetoelastic phononic crystals. *Applied Physics Letters*, **95**, 124104 (2009)

[9] Feng, R. and Liu, K. Tuning the band-gap of phononic crystals with an initial stress. *Physica B*, **407**, 2032–2036 (2012)

[10] Zhou, X. and Chen, C. Tuning the locally resonant phononic band structures of two-dimensional periodic electroactive composites. *Physica B*, **431**, 23–31 (2013)

[11] Su, X. L., Gao, Y. W., and Zhou, Y. H. The influence of material properties on the elastic band structures of one-dimensional functionally graded phononic crystals. *Journal of Applied Physics*, **112**, 123503 (2012)

[12] Wang, Y. Z., Li, F. M., Kishimoto, K., Wang, Y. S., and Huang, W. H. Wave localization in randomly disordered layered three-component phononic crystals with thermal effects. *Archive of Applied Mechanics*, **80**, 629–640 (2010)

[13] Senesi, M. and Ruzzene, M. Piezoelectric superlattices as multi-field internally resonating metamaterials. *AIP Advances*, **1**, 041504 (2011)

[14] Li, F. M. and Wang, Y. S. Study on wave localization in disordered periodic layered piezoelectric composite structures. *International Journal of Solids and Structures*, **42**, 6457–6474 (2005)

[15] Baz, A. Active control of periodic structures. *Journal of Vibration and Acoustics*, **123**, 472–479 (2001)

[16] Oh, J. H., Lee, I. K., Ma, P. S., and Kim, Y. Y. Active wave-guiding of piezoelectric phononic crystals. *Applied Physics Letters*, **99**, 083505 (2011)

[17] Wang, Y. Z., Li, F. M., Huang, W. H., Jiang, X. A., Wang, Y. S., and Kishimoto, K. Wave band gaps in two-dimensional piezoelectric/piezomagnetic phononic crystals. *International Journal of Solids and Structures*, **45**, 4203–4210 (2008)

[18] Wang, Y. Z., Li, F. M., Kishimoto, K., Wang, Y. S., and Huang, W. H. Band gaps of elastic waves in three-dimensional piezoelectric phononic crystals with initial stress. *European Journal of Mechanics A/Solids*, **29**, 182–189 (2010)

[19] Mikata, Y. Orthogonality condition for a multi-span beam and its application to transient vibration of a two-span beam. *Journal of Sound and Vibration*, **314**, 851–866 (2008)

[20] Gao, J. X. and Liao, W. H. Vibration analysis of simply supported beams with enhanced self-sensing active constrained layer damping treatments. *Journal of Sound and Vibration*, **280**, 329–357 (2005)

[21] Chen, L. W., Lin, C. Y., and Wang, C. C. Dynamic stability analysis and control of a composite beam with piezoelectric layers. *Composite Structures*, **56**, 97–109 (2002)

[22] Kim, H. W. and Kim, J. H. Effect of piezoelectric damping layers on the dynamic stability of plate under a thrust. *Journal of Sound and Vibration*, **284**, 597–612 (2005)

[23] Ramesh-Kumar, K. and Narayanan, S. Active vibration control of beams with optimal placement of piezoelectric sensor/actuator pairs. *Smart Materials and Structures*, **17**, 055008 (2008)

[24] Li, F. M., Chen, Z. B., and Cao, D. Q. Improving the aeroelastic flutter characteristics of supersonic beams using piezoelectric material. *Journal of Intelligent Material Systems and Structures*, **22**, 615–629 (2011)

[25] Li, F. M., Song, Z. G., and Chen, Z. B. Active vibration control of conical shells using piezoelectric materials. *Journal of Vibration and Control*, **18**, 2234–2256 (2012)

[26] Song, Z. G. and Li, F. M. Active aeroelastic flutter analysis and vibration control of supersonic beams using the piezoelectric actuator/sensor pairs. *Smart Materials and Structures*, **20**, 055013 (2011)

[27] Li, F. M., Kishimoto, K., Wang, Y. S., Chen, Z. B., and Huang, W. H. Vibration control of beams with active constrained layer damping. *Smart Materials and Structures*, **17**, 065036 (2008)

[28] Reddy, J. N. On laminated composite plates with integrated sensors and actuators. *Engineering Structures*, **21**, 568–593 (1999)

[29] Choi, S. C., Park, J. S., and Kim, J. H. Active damping of rotating composite thin-walled beams using MFC actuators and PVDF sensors. *Composite Structures*, **76**, 362–374 (2006)

[30] Raja, S., Pashilkar, A. A., Sreedeep, R., and Kamesh, J. V. Flutter control of a composite plate with piezoelectric multilayered actuators. *Aerospace Science and Technology*, **10**, 435–441 (2006)

[31] Mukherjee, A., Joshi, S. P., and Ganguli, A. Active vibration control of piezolaminated stiffened plates. *Composite Structures*, **55**, 435–443 (2002)

[32] Park, C. H. and Baz, A. Vibration control of bending modes of plates using active constrained layer damping. *Journal of Sound and Vibration*, **227**, 711–734 (1999)

[33] Lin, H. Y. and Tsai, Y. C. Free vibration analysis of a uniform multi-span beam carrying multiple spring-mass systems. *Journal of Sound and Vibration*, **302**, 442–456 (2007)